Maximizing the grafting of zwitterions onto the surface of ultrafiltration membranes to improve antifouling properties

Nima Shahkaramipour[a], Amin Jafari[a], Thien Tran[a], Christopher M. Stafford[b], Chong Cheng[a], and Haiqing Lin[*a]

[a]Department of Chemical and Biological Engineering, University at Buffalo, The State University of New York, Buffalo, NY 14260, USA.

[b]Materials Science & Engineering Division, National Institute of Standards and Technology (NIST), 100 Bureau Drive, Gaithersburg, MD 20899, USA.

*Corresponding author. Tel: +1-716-645-1856, Email: haiqingl@buffalo.edu

ABSTRACT

Superhydrophilic zwitterions have been extensively exploited for surface modification to improve antifouling properties. However, it remains challenging to form layers of < 20 nm with high zwitterion content on the surfaces with different degrees of hydrophilicity. We demonstrate that amine-functionalized sulfobetaine (SBAm) can be co-deposited with dopamine on ultrafiltration (UF) membranes, leading to a thickness of 10 nm to 50 nm and an SBAm content of up to 31 mass% in the coating layers. The covalently grafted SBAm is stable underwater and improves the antifouling properties, as evidenced by the lower trans-membrane pressure required to retain targeted water fluxes than that required for the pristine membranes. The SBAm is also more effective than conventionally used sulfobetaine methacrylate (SBMA) for the zwitterion grafting on the surface to improve antifouling properties.

Keywords: Membranes for water purification; Surface modification; Dopamine; Zwitterions; Antifouling properties

1. Introduction

Polymeric membranes are widely employed for wastewater treatment due to their superior separation performance and high energy-efficiency. However, membranes are often susceptible to fouling by accumulation of suspended solids and dissolved contaminants, which decreases water permeance [1-3]. An effective strategy to mitigate fouling is to graft hydrophilic materials onto the membrane surface to minimize any favorable interactions between the surface and foulants, such as zwitterions containing cations and anions with neutral charges but superhydrophilicity. For example, zwitterionic materials (ZMs) with acrylate and methacrylate groups were directly copolymerized with membrane materials [4], deposited on the surface using chemical vapor deposition [5], or grafted from the surface using surface-initiated polymerization [6-8] or other reactions with the surface [9-13]. However, these processes can involve complex chemistry and are often surface-specific. There is a need for a versatile platform to graft various zwitterions on-demand for different foulants onto membranes with different surface properties.

Bio-inspired dopamine can self-polymerize in aqueous solutions and form insoluble polydopamine (PDA) that can deposit on hydrophilic and hydrophobic polymer surfaces [14, 15]. More importantly, the “adhesive” PDA comprises catechol and amine groups and can be used to incorporate functional ZMs [16-19]. For example, poly(sulfobetaine methacrylate) (polySBMA) can be directly coated on a membrane surface primed by PDA through non-covalent linkages [20-22]. However, the lack of covalent bonds between the PDA and superhydrophilic ZMs presents concerns for long-term underwater operation.

The key to graft ZMs using dopamine is to optimize the functional groups of the ZMs that can react with PDA to obtain thin layers (without adding significant transport resistance) and high zwitterion content to maximize antifouling properties. Methacrylate-containing ZMs have been

co-deposited with dopamine, such as sulfobetaine methacrylate (SBMA), with good stability and hydrophilicity [18, 19, 23]. When 1 g/L dopamine and 4 g/L SBMA was deposited for 8 h (i.e. 4-SBMA/1-Dopa@8h), the SBMA content in the coating layer was only ≈ 11 mass%, and increasing the SBMA content from 0 g/L to 4 g/L in the solution had minimal effect on the layer thickness (≈15 nm). By contrast, for *y*-SBMA/2-Dopa@8h, increasing the SBMA content (*y*) from 0 g/L to 30 g/L increased the coating layer thickness from ≈32 nm to ≈59 nm, and the SBMA content in the coating layer was observed to be as high as 34 mass% [19]. However, thick surface layers are not preferred for membrane modification due to the increased resistance for water transport, though it has not been systematically explored to date.

Conversely, amine-containing materials can be co-deposited with dopamine [14, 24-26]. For example, amine-terminated poly(ethylene glycol) (PEG-NH_2) was grafted onto PDA-functionalized ultrafiltration (UF) membranes and formed a layer of ≈300 nm [27]. 4,4'-Azodianiline (AZO) was similarly grafted onto PDA-functionalized membranes to form a layer of 17 to 37 nm [28]. Alternatively, polyethylenimine (PEI) was co-deposited with dopamine to produce nanofiltration (NF) membranes for desalination [29]. However, amine-functionalized ZMs have not been co-deposited with dopamine on the membrane surface and explored for improving antifouling properties.

Herein we demonstrate that sulfobetaine amine (SBAm) can be co-deposited with dopamine onto the surface of a UF membrane, producing thin layers and high zwitterion content that display superior antifouling properties. As shown in Fig. 1, SBAm can react with dopamine monomer/oligomer and thus be incorporated into a stable PDA layer, which is thin and does not significantly block the membrane pores. The products of the SBAm and dopamine in the solutions were analyzed using ^{1}H NMR and scanning electron microscopy (SEM). The effects of coating

conditions (including the composition of coating solutions and coating time) on the thickness and the SBAm content of the coating layer were determined. The optimally modified membranes with a thin layer and high SBAm content were challenged with a model foulant and compared with the pristine membranes and those modified using SBMA.

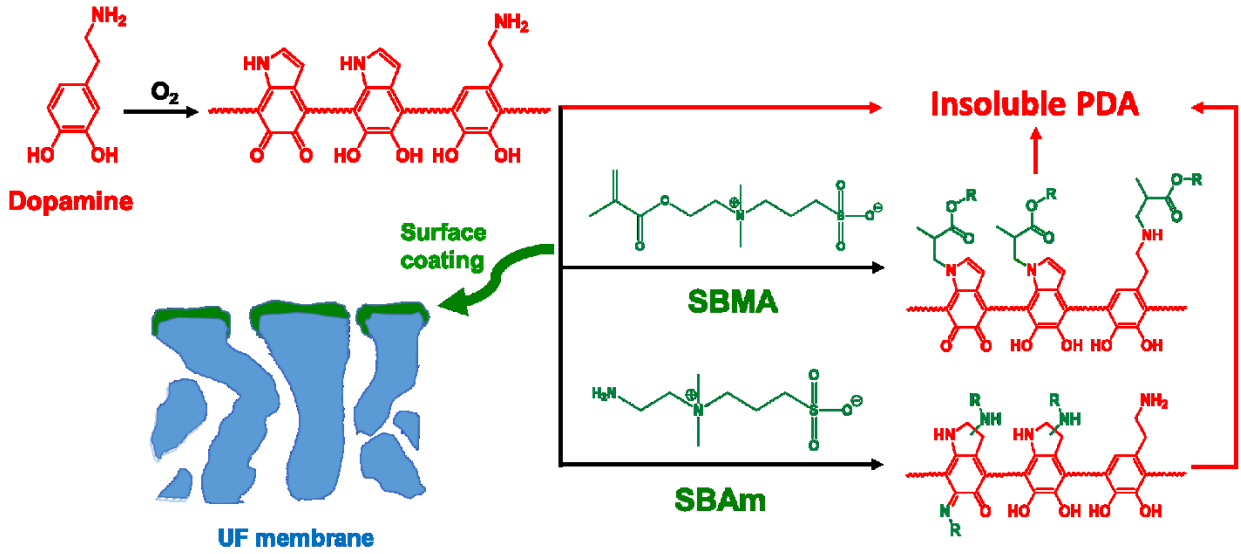

Fig. 1. Reactions between dopamine and methacrylate or amine-containing ZMs used in this study, and schematic of coating ZMs+PDA onto a UF membrane. R = $-CH_2CH_2N^+(CH_3)_2CH_2CH_2CH_2SO_3^-$ [24, 30, 31].

2. Experimental

2.1. Materials

Dopamine hydrochloride, Trizma base (Tris), SBMA, deuterium oxide (D_2O), and sodium alginate (from brown algae) were purchased from Sigma-Aldrich (St. Louis, MO). SBAm and ethanol were procured from eNovation Chemicals (Green Brook, NJ) and Fisher Scientific (Waltham, MA), respectively. A polysulfone UF membrane (PSf-25) was purchased from Alfa-Laval (Warminster, PA) [32].

2.2. Surface modification

The coating of the substrates (including polystyrene wells, silicon wafers, and membranes) follows the procedures described in the literature [17, 18]. The steps are briefly described here using an example of PSf-25 membranes. First, a membrane sheet (5" x 6") was pretreated by soaking in ethanol for 24 h followed by Milli-Q water. Second, the membrane was secured with a rubber gasket, a plastic frame, and binder clips, and the assembly was placed on a rocking platform shaker (VWR International, Radnor, PA). Third, an aqueous solution (25 mL) containing desirable contents of dopamine, ZM, and Tris was poured onto the top of the membrane, and the shaker was turned on for the membrane surface to be exposed to the solution and air alternatively. After the desired time, the coating solution was poured away, and the coated membrane was rinsed under running water and kept in water overnight before testing.

The coated samples are denoted as *y*-ZM/*x*-Dopa@*z*h, where *y* and *x* represent the concentration of ZM (SBMA or SBAm) and dopamine in the coating solution (g/L), respectively, and *z* is the coating time (h).

2.3 Characterization of coating solutions and layers

The coating solutions were characterized using a Varian INOVA-500 ^{1}H NMR spectrometer (Varian Medical Systems, Palo Alto, CA) with D_2O as the solvent. Additionally, the solutions were drop-cast onto wafers, and the dried aggregates were examined using a focused-ion beam SEM (FIB-SEM, Auriga, ZEISS International, Germany) and attenuated total reflectance Fourier-transform infrared spectrometer (ATR-FTIR, Vertex 70, Bruker, MA).

Water contact angles were determined using a Ramé Hart goniometer (Model 190, Succasunna, NJ) and 10 μL water droplets through the well-recognized sessile drop technique [6, 33-36]. Five measurements were recorded for each sample. Though the captive bubble method provides a better reflection on operating conditions than the sessile drop method, both methods

have shown the same trend in understanding the change in surface hydrophilicity [18]. The coating layer thickness of the modified polystyrene wells were measured via a Filmetrics F20 thin film measurement instrument (Filmetrics, Inc., San Diego, CA). The refractive index value of PDA, SBMA, SBAm is assumed to be 1.60 [17, 18], 1.37 [18, 37], and 1.37, respectively. X-ray photoelectron spectroscopy (XPS) was used for elemental analysis of the coated wafers with a Kratos AXIS Ultra DLD Spectrometer (Kratos Analytical, Manchester, UK). The spectra were collected from spot sizes of 300 μm × 700 μm and analyzed using the CasaXPS software package [32].

2.4. Membrane characterization

Pure-water permeance (A_W in L m^{-2} h^{-1} bar^{-1} or LMH/bar) of the membranes was determined using dead-end cells (Sterlitech, Kent, WA) and calculated using the following equation:

$$A_w = \frac{J_W}{\Delta p} = \frac{dV}{dt}\frac{1}{\Delta p A_m} \quad (1)$$

where J_W is the water flux (LMH), Δp is the trans-membrane pressure (TMP, bar), A_m is the active membrane area (m^2), and dV/dt is the volumetric flow rate (L/h). For each membrane, the average permeance of six stamps is reported.

The molecular weight cutoffs (MWCO) [38] of the membranes were determined using PEG with various mass average molar masses including (1, 2, 4, 10, and 20) kDa. The MWCO is conventionally defined as the lowest molecular weight that is rejected by the membrane at a level of 90 %. The rejection of the PEG (R, %) can be calculated using the following equation:

$$R = \left(1 - \frac{C_p}{C_f}\right) \times 100\% \quad (2)$$

where C_p and C_f are the PEG concentration in the permeate and feed, respectively. Both C_p and C_f were determined using a total organic carbon analyzer (Shimadzu, Japan). The membrane pore size can be estimated as the Stokes radius (a, nm) of the corresponding PEG molecule [21, 39]:

$$a = 16.73 \times 10^{-3} {M_W}^{0.557} \quad (3)$$

The antifouling properties of the UF membranes were characterized using sodium alginate as a model foulant in both a dead-end filtration and a constant-flux crossflow geometry [40, 41]. For dead-end cells, a constant feed pressure was applied, and the decreased water permeance was recorded. For the constant-flux system, the feed pressure was kept constant while the permeate pressure was decreased to maintain a defined flux. The resistance to water permeation (R_W, m^{-1}) can be calculated using Eq. 4 [42]:

$$R_W = \frac{\Delta p}{\mu_W J_W} \quad (4)$$

where μ_W is the water viscosity. Membrane fouling is often characterized by the relative resistance defined as the ratio of the resistance at any time to the initial pure water value.

3. Results and discussion

3.1. Reaction between the ZMs and dopamine in solutions

To elucidate the reaction of SBAm and dopamine in solutions, Fig. 2a compares ^{1}H NMR spectra of dopamine, SBAm, 1-Dopa@16h, and 5-SBAm/1-Dopa@16h in D_2O. The dopamine solution was kept oxygen-free to avoid the formation of PDA, and the spectrum shows characteristic peaks at (6.6 to 6.8) ppm corresponding to the aromatic protons of dopamine, and 2.7 ppm and 3 ppm for $NH_2CH_2CH_2$ and $NH_2CH_2CH_2$, respectively. By contrast, these peaks disappear in 1-Dopa@16h, confirming the formation of insoluble PDA in the presence of O_2. The peak at ≈3.2 ppm belongs to the Tris buffer, which was used to maintain the pH of polymerization.

However, 5-SBAm/1-Dopa@16h shows characteristic peaks for aromatic protons (in the gray inserted figure), suggesting the formation of soluble intermediate chemicals (cf. Fig. 1) through reaction of the amine group of SBAm with the catechol moieties of dopamine monomer/oligomer via Michael addition and with the vinyl groups of dopamine monomer/oligomer via Schiff base reaction [30]. The same trend is observed for 25-SBAm/1-Dopa@16h (see Fig. S1a). The slight shift of the peak for the Tris buffer in 25-SBAm/1-Dopa compared with 1-Dopa can be attributed to the change in the molecular environment. The 5-SBAm/1-Dopa@16h solution was further dialyzed using membranes with an MWCO of 3.5 kDa for three days, and all the peaks disappear, suggesting that the soluble chemicals have molar mass less than 3.5 kDa assuming minimal adsorption of the chemicals on the dialysis membranes.

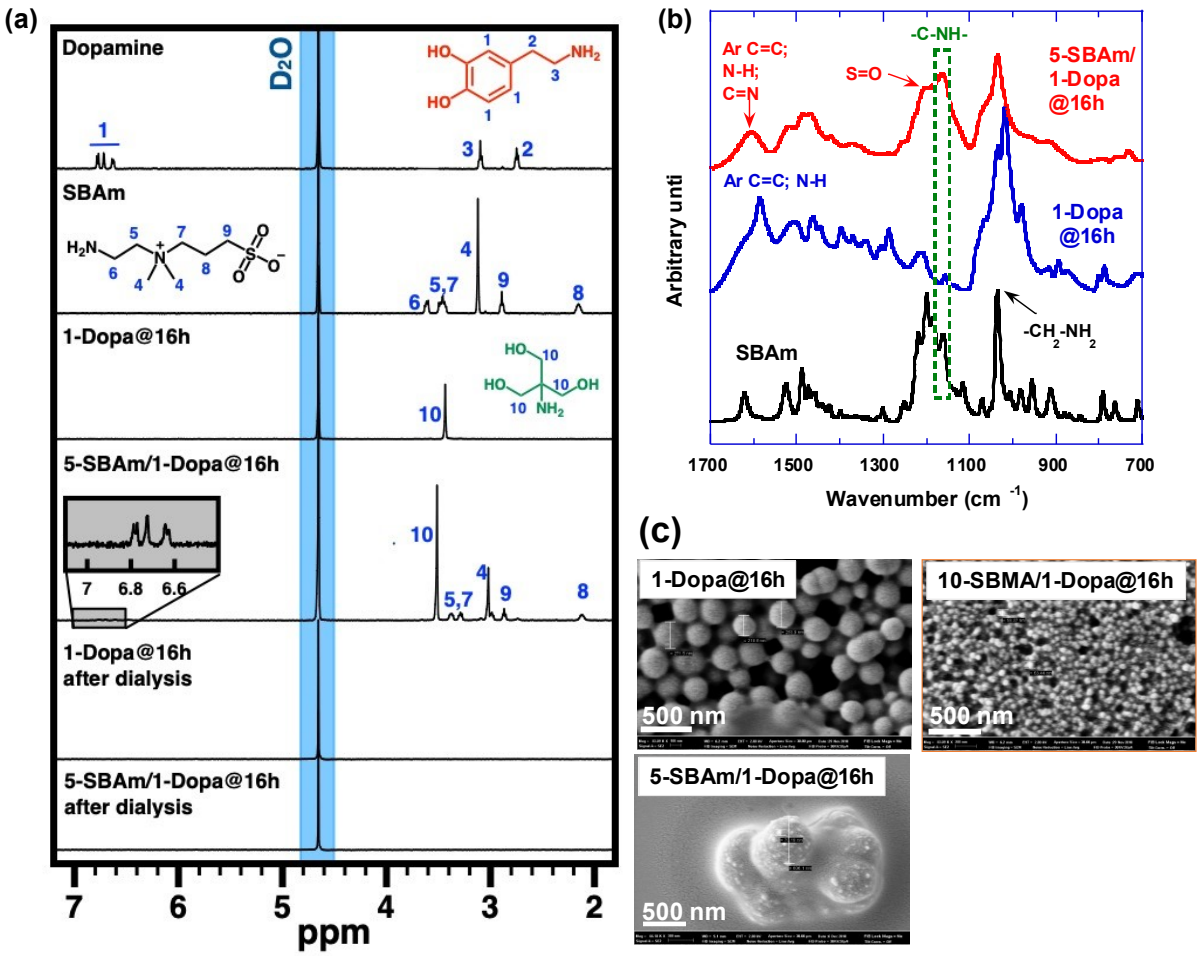

Fig. 2. (a) ^{1}H NMR spectra of dopamine, SBAm, 1-Dopa@16h, and 5-SBAm/1-Dopa@16h in D_2O. The latter two were also dialyzed using a membrane with a MWCO of 3.5 kDa. The gray inserted figure shows the aromatic protons from dopamine and soluble SBAm/PDA product. (b) FTIR spectra of SBAm and dried aggregates of 1-Dopa@16h and 5-SBAm/1-Dopa@16h. (c) SEM images of the dried PDA and ZM/PDA aggregates.

Fig. 2b exhibits the FTIR spectra for SBAm and dried aggregates from the 1-Dopa@16h and 5-SBAm/1-Dopa@16h solutions. SBAm exhibits characteristic peaks of 1050 cm^{-1} for C-N stretch corresponding to the primary amine and 1160 cm^{-1} for S=O stretch of the sulfonate. The 1-Dopa@16h displays a peak at 1585 cm^{-1} for aromatic C=C stretch and N-H bending [18, 22]; with the presence of C=N stretch as a result of Schiff base reaction [30], the peak shifts to 1605 cm^{-1} for 5-SBAm/1-Dopa@16h. Compared with 1-Dopa@16h, 5-SBAm/1-Dopa@16h shows a strong

peak at ≈1150 cm^{-1} ascribed to –C-NH- stretch, confirming the Michael addition between SBAm and dopamine monomer/oligomer [18, 19, 26].

Fig. 2c compares the SEM photos of the dried aggregates of 1-Dopa@16h, 10-SBMA/1-Dopa@16h, and 5-SBAm/1-Dopa@16h. The 1-Dopa@16h shows nanoparticle size of ≈260 nm, while the particle size increases with the introduction of SBAm (≈650 nm) and decreases with the introduction of SBMA (≈60 nm), suggesting the reaction between dopamine monomer/oligomer and SBAm/SBMA in the solutions. The increased particle size with adding SBAm is also confirmed by additional SEM images (cf. Fig. S1b) and dynamic light scattering (DLS) measurements (cf. Fig. S1c).

3.2. Characterization of coating layers

Fig. 3a displays the effect of the ZM content in the coating solution (y) on the thickness of the coating layer (y-ZM/1- Dopa@16h) in polystyrene wells, which serve as indicators for polymeric membranes assuming that the coating layer on polystyrene would be similar to that on polymeric membranes. Direct thickness measurement of the modified membranes using F-20 is not feasible because the uncovered porous substrate interferes with the signal [18]. Increasing the ZM content increases the coating layer thickness before decreasing. For example, as the SBAm content increases from 0 to 5 g/L and 25 g/L, the thickness increases from 21 nm ± 3 nm to 45 nm ± 4 nm before decreasing to 16 nm ± 5 nm. At high ZM contents, the reaction between dopamine monomer/oligomer and ZM competes with the PDA formation, decreasing the layer thickness. Similar trends have been reported for SBMA [19]. The layer thickness reaches a maximum at y values of 10 g/L for SBMA and 5 g/L for SBAm, and these conditions were chosen for further studies. Though the coating time of 16 h is long, the goal of this study is to determine the effect of

surface chemistry on antifouling properties. Once such an understanding becomes available, the kinetics of the dopamine polymerization may be accelerated to accelerate the surface modification.

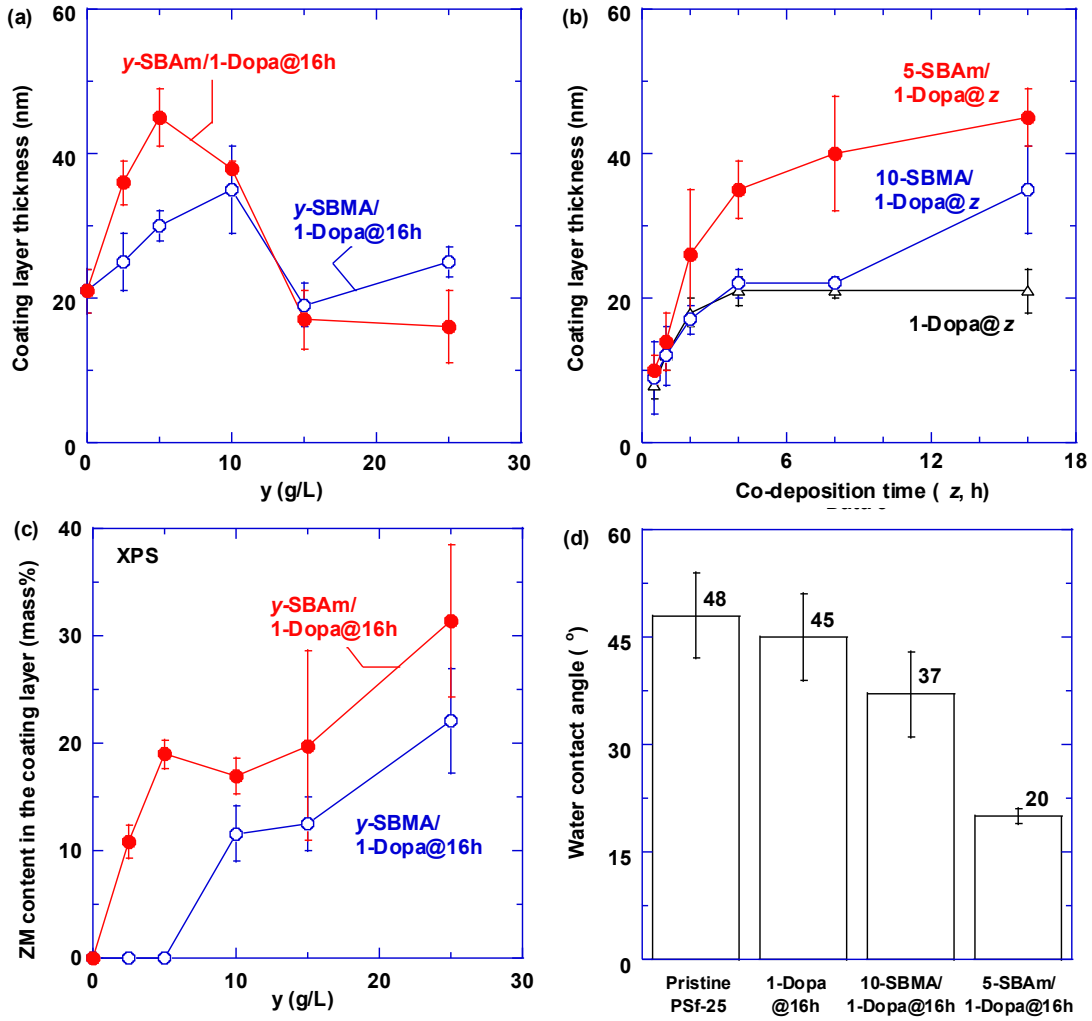

Fig. 3. (a) Effect of the ZM content in the coating solutions (y, g/L) on the coating layer thickness when cast in polystyrene wells for y-ZM/1-Dopa@16h; (b) effect of the co-deposition time (z, h) on the coating layer thickness for 1-Dopa, 10-SBMA/1-Dopa, and 5-SBAm/1-Dopa; (c) comparison of the ZM content in the coating layer on the silicon wafers for y-ZM/1-Dopa@16h as a function of ZM content in the coating solutions (y, g/L); and (d) effect of representative surface modification on the water contact angle of UF membranes. The error bars represent one standard deviation of the data and are taken as the uncertainty of the measurements.

Increasing the co-deposition time (z) increases the coating layer thickness before leveling off for 10-SBMA/1-Dopa and 5-SBAm/1-Dopa, as shown in Fig. 3b. The co-deposition time above

16 h is not investigated in this study to avoid excessively long time of modification. SBAm leads to thicker coating layers than SBMA, indicating that amine groups are more effective than methacrylate groups in grafting the zwitterion to the dopamine.

Fig. 3c shows the ZM content in the coating layer on the wafers determined using XPS, which was calculated from the atomic compositions (cf. Table S1 and Eq. S1). Typical spectra for a bare silicon wafer, PDA-coated Si, and SBAm/PDA-coated Si are shown in Fig. S2. Increasing the *y* value continuously increases the ZM content, in contrast to the trend of the coating layer thickness (which peaks at certain *y* values). On the other hand, both effects are desirable for membrane surface modification, i.e. thinner and more hydrophilic coating to achieve antifouling properties without dramatically increasing transport resistance. SBAm deposits more readily than SBMA in the coating layer. For example, at y = 25 g/L, the coating layer has 31 mass% SBAm and only 22 mass% SBMA, corresponding to 25 mass% and 13 mass% zwitterionic groups (i.e. $-N^{+}(CH_3)_2CH_2CH_2CH_2SO_3^{-}$), respectively.

The ZM grafting on the membranes decreases the water contact angle (cf. Fig. 3d), indicating improved hydrophilicity, which is consistent with the thicker layer and higher ZM content for the SBAm grafting.

3.3. Effect of surface modification on membrane performance

Fig. 4a illustrates the rejection curves as a function of PEG molar mass for the pristine and modified PSf-25 UF membranes. The pristine PSf-25 membrane shows a MWCO of 17.5 kDa, which is comparable with that (25 kDa) given by the manufacturer, while the MWCO decreases to 8.7 kDa for 10-SBMA/1-Dopa@16h and 7.5 kDa for 5-SBAm/1-Dopa@16h. Accordingly, the nominal pore size decreases from 3.9 nm to 2.6 nm for 10-SBMA/1-Dopa@16h and 2.4 nm for 5-

SBAm/1-Dopa@16h. The decreasing order of the pore size is consistent with the thickness increase of the coating layer.

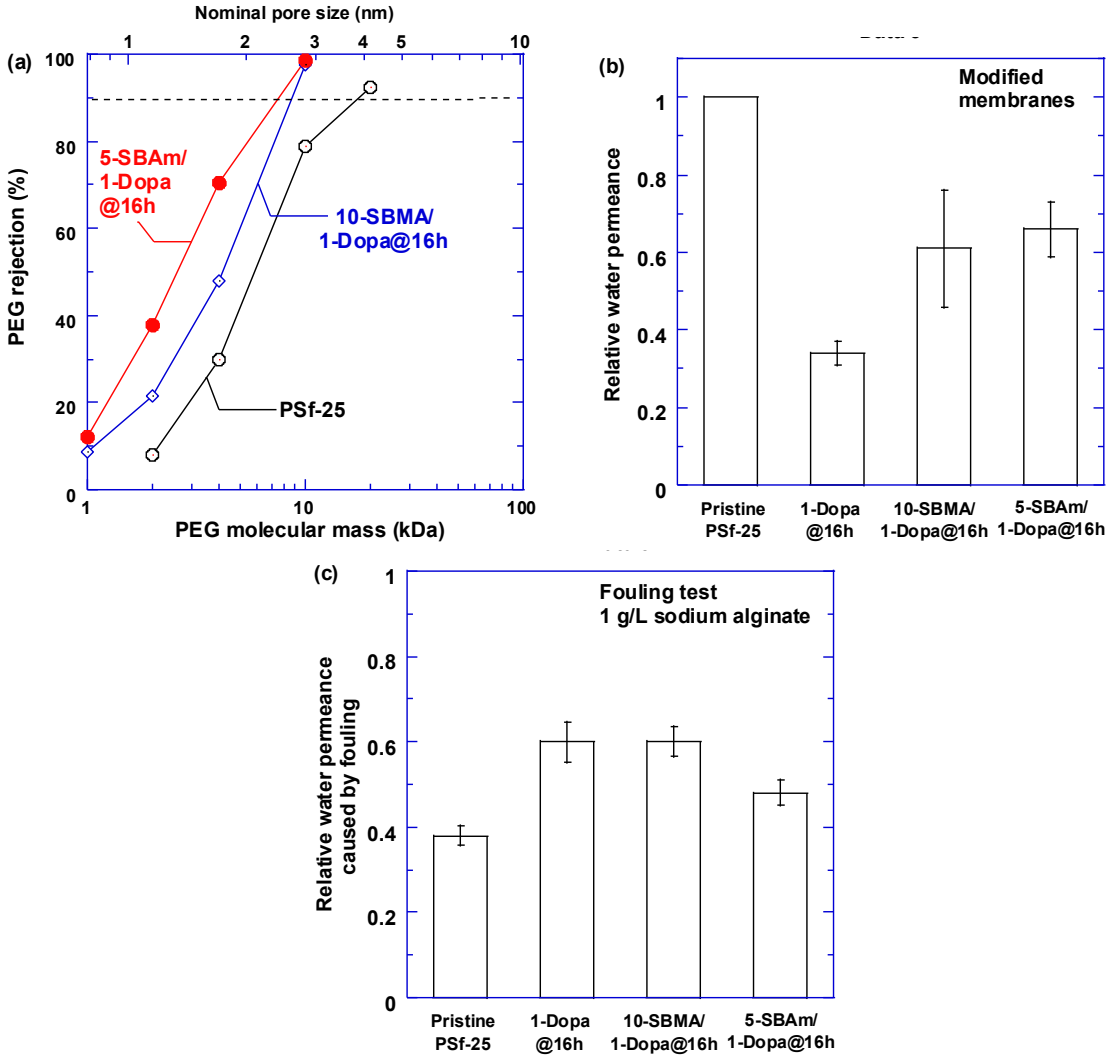

Fig. 4. Effect of surface modification on (a) PEG rejection curves as a function of the PEG M_W and (b) the relative water permeance (defined as the pure water permeance ratio of the modified membrane to the pristine one), and (c) the water permeance reduction percentage when challenged with a 1 g/L sodium alginate solution. For Fig. 4b, the error bars represent one standard deviation of the data. For Fig. 4c, the uncertainty is estimated using an error propagation method [43].

Surface modification often decreases water permeance because of the increased resistance to water transport. Fig. 4b shows that the relative water permeance (defined as the permeance ratio of the modified membrane to the pristine one) is below 1, indicating increased resistance to water

permeation. Interestingly, compared with 1-Dopa@16h, adding ZMs increases water permeance due to the improved hydrophilicity. Fig. 4c illustrates the effect of surface modification on the antifouling properties when challenged by 1 g/L sodium alginate solution. Sodium alginate is a model biopolymer mimicking polysaccharides and a vital element in the formation of biofilms. Therefore, it has been widely used as a model fouling to investigate the fouling of membranes for water purification [44-51]. The modified membranes exhibit a relative water permeance caused by the fouling (defined as the ratio of permeance during the fouling test to that with pure water) ranging from 0.48 to 0.60, greater than the pristine one (0.38), confirming the improved antifouling properties by PDA and ZM coating.

Industrial membranes are often operated at a constant flux (for stable productivity) at or slightly below the threshold flux (J_{TH}, defined as the flux above which significant fouling occurs) [42, 52]. Fig. 5a illustrates the flux stepping method to obtain J_{TH} for 25-SBAm/1-Dopa@16h with 2 g/L sodium alginate solution. During the test, each flux was held for 10 min while continuously recording the TMP. Fig. 5b shows the average TMP as a function of the water flux. Three linear regions are considered with an $R^2 > 0.99$. The intersection between the second and third region is defined as the J_{TH}, while the intersection between the first and second region is the critical flux (J_C, the flux below which the fouling rate is negligible) [21]. In these measurements, the pristine and modified membranes were tested in series to provide direct comparison of their antifouling properties and avoid interference from some operating errors such as flow rates, feed conditions, etc.

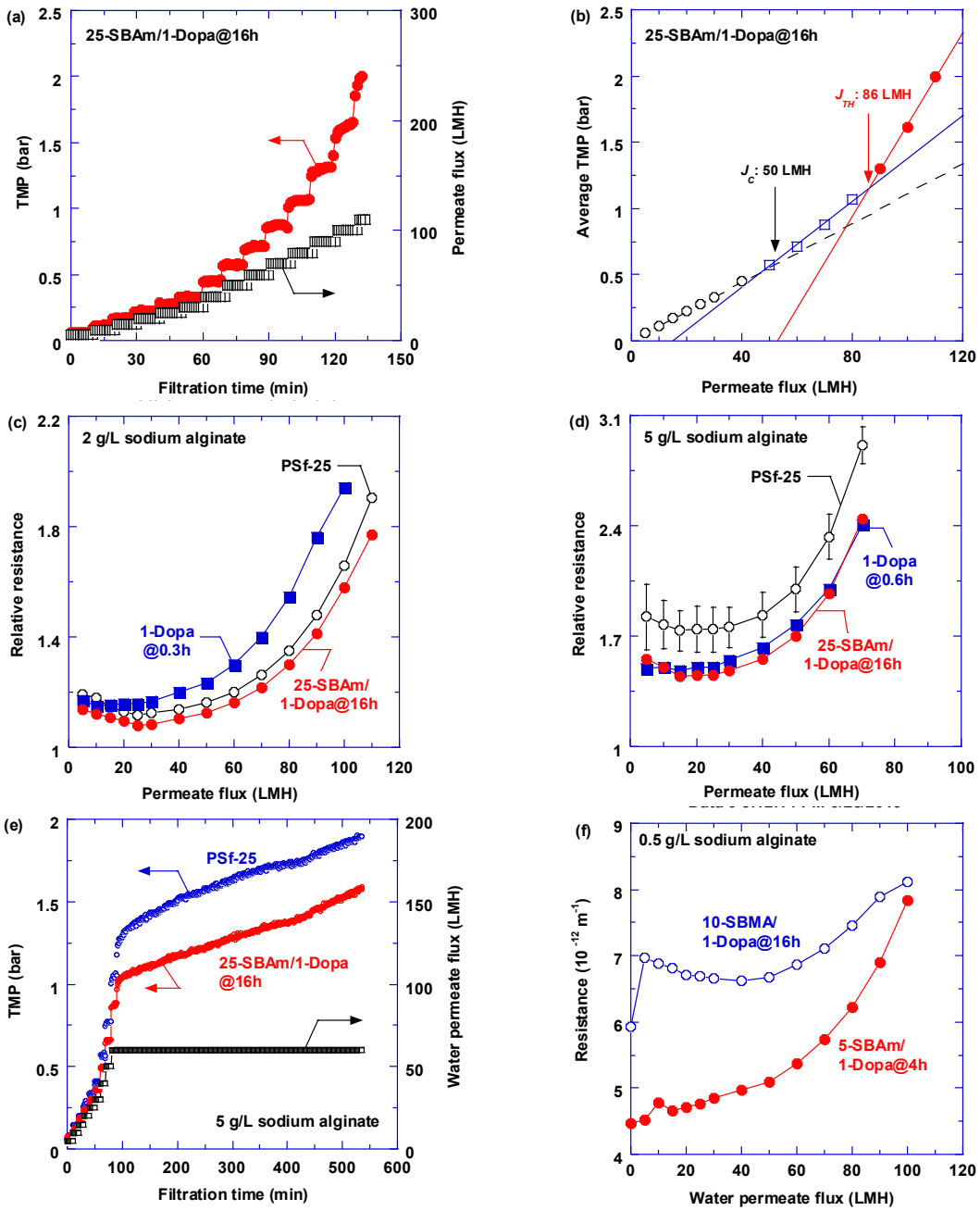

Fig. 5. (a) Flux-stepping experiment and (b) determination of the critical and threshold flux for 25-SBAm/1-Dopa@16h examined with 2 g/L sodium alginate. Effect of the permeate flux on the relative resistance with (c) 2 g/L and (d) 5 g/L sodium alginate for three membranes, PSf-25, 1-Dopa@*z*h, and 25-SBAm/1-Dopa@16h. (e) Flux stepping and long-term fouling experiments for PSf-25 and 25-SBAm/1-Dopa@16h using a 5 g/L sodium alginate. (f) Effect of the permeate flux on the resistance with 0.5 g/L sodium alginate in two membranes, 5-SBAm/1-Dopa@4h, and 10-SBMA/1-Dopa@16h. The feed pressure was 2.4 barg (0.24 MPa), and the Reynolds number was ≈1600. The error bars in (d) represent the standard deviations of four samples of PSf-25. For the other membranes, the uncertainty is estimated to be ≈12% for the resistance using the error

propagation method with an uncertainty of 0.002 bar for TMP, 0.0006 L/h for permeate flow, and ≈10% for water permeance due to the sample variance [43].

Fig. 5c compares the fouling behavior of three membranes, PSf-25, 1-Dopa@0.3h, and 25-SBAm/1-Dopa@16h, which show comparable pure-water permeance of (106, 97, and 99) LMH/bar, respectively, and comparable J_{TH} values of (86, 68, and 86) LMH/bar (cf. Fig. S3), respectively. Therefore, a comparison of these membranes can provide useful information regarding the impact of surface modification on the antifouling properties. At fluxes below J_C, the relative resistance does not change for all three membranes (cf. Fig. 5c) because of the negligible fouling. At higher fluxes, the relative resistance increases with increasing water flux, and the increasing rate of resistance becomes more rapid due to the increasingly severe fouling. The membrane modified by SBAm shows the lowest relative resistance, confirming the benefit of the SBAm in improving the antifouling properties. Fig. 5d compares the relative resistance at 5 g/L sodium alginate in the pristine PSf-25 and membranes modified by 1-Dopa@0.6h and 25-SBAm/1-Dopa@16h. Both modified membranes show significantly lower relative resistance than the PSf-25, which can be ascribed by the improved hydrophilicity caused by the zwitterion grafting. The surface modification inevitably increases the surface roughness compared with the pristine membrane [20]. However, the surface roughness of the modified membranes cannot be directly determined because of the porous nature, and its effect on the fouling resistance cannot be elucidated. Therefore, the fouling resistance is often correlated with the surface hydrophilicity for most of the studies on the PDA modification [18, 20, 39, 52].

The long-term performance of the membranes when challenged with 5 g/L sodium alginate solution is illustrated in Fig. 5e. The PSf-25 and 25-SBAm/1-Dopa@16h exhibit pure-water permeance of 146 LMH/bar and 138 LMH/bar, respectively, making them ideal for comparison.

At the initial flux-stepping stage, the SBAm-modified membrane exhibits 15 % to 25 % lower resistance than the pristine one. During the continuing test of ≈8 h at 60 LMH, the SBAm-modified membrane again shows lower resistance, confirming the stability and improved antifouling properties of the surface modification. The superior antifouling behavior of the SBAm-modified membrane over the PDA-modified one is also demonstrated in Fig. S3d. Considering the storage of these modified membranes in water for several day before the tests, these results suggest that the coating layers are stable in water during those days, which is consistent with those reported in the literature (i.e., stable for several weeks or even months) [18, 22, 53].

Fig. 5f compares the antifouling properties of 10-SBMA/1-Dopa@16h and 5-SBAm/1-Dopa@4h with 0.5 g/L sodium alginate solution. Despite the same coating layer thickness of both coatings (i.e. 35 nm, as shown in Fig. 3b), the SBAm-modified membrane exhibits lower resistance than the SBMA-modified one, though the difference diminishes as the flux increases above J_{TH}. Such a result demonstrates that SBAm is more effective than SBMA for surface-grafting to enhance antifouling properties.

4. Conclusions

We demonstrate a facile approach to graft zwitterions (up to 31 mass% in thin layers of < 20 nm) on the membrane surface to improve antifouling properties. The amine-functionalized ZMs (i.e. SBAm) can be co-deposited with dopamine on a variety of surfaces in aqueous solution at ≈ 22 °C. The reaction between SBAm and dopamine monomer/oligomer is confirmed by ^{1}H NMR spectroscopy and FTIR. The grafting of the zwitterions in the coating layers is also confirmed by XPS. SBAm leads to a thicker coating layer and higher zwitterion content than SBMA, suggesting that amine groups are more effective than methacrylate counterparts to graft zwitterions. In a

constant-flux system, SBAm-modified membranes show 15 % to 25 % lower resistance to water permeation than the SBMA-modified analog and pristine one, confirming the effectiveness of the grafting of amine-functionalized zwitterions to enhance membrane antifouling properties.

Declaration of interest

The authors declare no conflicts of interest.

Acknowledgments

We acknowledge the financial support from the U.S. National Science Foundation (NSF Award No. 1635026) and Department of Energy Small Business Innovation Research program (Award No. DE-SC-0017077). This work is an official contribution of the National Institute of Standards and Technology and not subject to copyright in the United States.

References

[1] D. Miller, D. Dreyer, C. Bielawski, D. Paul, B. Freeman. Surface modification of water purification membranes: A review. Angew. Chem. Int. Ed. 56 (2017) 4662-4711.

[2] N. Shahkaramipour, T. Tran, S. Ramanan, H. Lin. Membranes with surface enhanced antifouling properties for water purification. Membranes. 7 (2017) 13.

[3] R. Zhang, Y. Liu, M. He, Y. Su, X. Zhao, M. Elimelech, Z. Jiang. Antifouling membranes for sustainable water purification: strategies and mechanisms. Chem. Soc. Rev. 45 (2016) 5888-5924.

[4] P. Kaner, A. V. Dudchenko, M. S. Mauter, A. Asatekin. Zwitterionic copolymer additive architecture affects membrane performance: fouling resistance and surface rearrangement in saline solutions. J. Mater. Chem. A. 7 (2019) 4829-4846.

[5] R. Yang, P. Moni, K. K. Gleason. Ultrathin zwitterionic coatings for roughness-independent underwater superoleophobicity and gravity-driven oil–water separation. Adv. Mater. Interfaces. 2 (2015) 1400489.

[6] D. Hong, H.-C. Hung, K. Wu, X. Lin, F. Sun, P. Zhang, S. Liu, K. E. Cook, S. Jiang. Achieving ultralow fouling under ambient conditions via surface-initiated ARGET ATRP of carboxybetaine. ACS Appl. Mater. Interf. 9 (2017) 9255-9259.

[7] Z. Liu, Q. Jiang, Z. Jin, Z. Sun, W. Ma, Y. Wang. Understanding the antifouling mechanism of zwitterionic monomer grafted PVDF membranes: A comparative

experimental and molecular dynamics simulation study. ACS Appl. Mater. Interf. 11 (2019) 14408−14417.
[8] D. M. Davenport, J. Lee, M. Elimelech. Efficacy of antifouling modification of ultrafiltration membranes by grafting zwitterionic polymer brushes. Sep. Purif. Technol. 189 (2017) 389-398.
[9] Q. Li, J. Imbrogno, G. Belfort, X. L. Wang. Making polymeric membranes antifouling via "grafting from" polymerization of zwitterions. J. Appl. Polym. Sci. 132 (2015) 41781.
[10] Y.-H. Chiao, A. Sengupta, S.-T. Chen, S.-H. Huang, C.-C. Hu, W.-S. Hung, Y. Chang, X. Qian, S. R. Wickramasinghe, K.-R. Lee. Zwitterion augmented polyamide membrane for improved forward osmosis performance with significant antifouling characteristics. Sep. Purif. Technol. 212 (2019) 316-325.
[11] M. Yi, C. H. Lau, S. Xiong, W.-J. Wei, R.-Z. Liao, L. Shen, A. Lu, Y. Wang. Zwitterion-Ag complexes that simultaneously enhance biofouling resistance and silver binding capability of thin film composite membranes. ACS Appl. Mater. Interf. 11 (2019) 15698−15708.
[12] H. Sun, Y. Zhang, H. Sadam, J. Ma, Y. Bai, X. Shen, J.-K. Kim, L. Shao. Novel mussel-inspired zwitterionic hydrophilic polymer to boost membrane water-treatment performance. J. Membr. Sci. 582 (2019) 1-8.
[13] N. Ma, J. Cao, H. Li, Y. Zhang, H. Wang, J. Meng. Surface grafting of zwitterionic and PEGylated cross-linked polymers toward PVDF membranes with ultralow protein adsorption. Polymer. 167 (2019) 1-12.
[14] H. Lee, S. M. Dellatore, W. M. Miller, P. B. Messersmith. Mussel-inspired surface chemistry for multifunctional coatings. Science. 318 (2007) 426-430.
[15] D. R. Dreyer, D. J. Miller, B. D. Freeman, D. R. Paul, C. W. Bielawski. Perspectives on poly(dopamine). Chem. Sci. 4 (2013) 3796-3802.
[16] W. Qiu, H. Yang, Z. Xu. Dopamine-assisted co-deposition: An emerging and promising strategy for surface modification. Adv. Colloid Interface Sci. 256 (2018) 111-125.
[17] N. Shahkaramipour, C. K. Lai, S. R. Venna, H. Sun, C. Cheng, H. Lin. Membrane surface modification using thiol-containing zwitterionic polymers via bioadhesive polydopamine. Ind. Eng. Chem. Res. 57 (2018) 2336-2345.
[18] N. Shahkaramipour, S. N. Ramanan, D. R. Fister, E. Park, S. R. Venna, H. Sun, C. Cheng, H. Lin. Facile grafting of zwitterions onto membrane surface to enhance antifouling properties for wastewater reuse. Ind. Eng. Chem. Res. 56 (2017) 9202−9212.
[19] C. Zhang, M. Ma, T. Chen, H. Zhang, D. Hu, B. Wu, J. Ji, Z. Xu. Dopamine-triggered one-step polymerization and codeposition of acrylate monomers for functional coatings. ACS Appl. Mater. Interf. 9 (2017) 34356-34366.
[20] C. Chang, K. W. Kolewe, Y. Li, K. I., B. D. Freeman, K. R. Carter, J. D. Schiffman, T. Emrick. Underwater superoleophobic surfaces prepared from polymer zwitterion/dopamine composite coatings. Adv. Mater. Interfaces. 3 (2016) 1500521.
[21] A. Kirschner, C. Chang, S. Kasemset, T. Emrick, B. D. Freeman. Fouling-resistant ultrafiltration membranes prepared via co-deposition of dopamine/zwitterion composite coatings. J. Membr. Sci. 541 (2017) 300-311.
[22] R. Zhou, P. Ren, H. Yang, Z. Xu. Fabrication of antifouling membrane surface by poly(sulfobetaine methacrylate)/polydopamine co-deposition. J. Membr. Sci. 466 (2014) 18-25.

[23] C.-Y. Liu, C.-J. Huang. Functionalization of polydopamine via the aza-michael reaction for antimicrobial interfaces. Langmuir. 32 (2016) 5019-5028.
[24] W. Qiu, G. Wu, Z. Xu. Robust coatings via catechol–amine codeposition: Mechanism, kinetics, and application. ACS Appl. Mater. Interf. 10 (2018) 5902-5908.
[25] W. Qiu, H. Yang, L. Wan, Z. Xu. Co-deposition of catechol/polyethyleneimine on porous membranes for efficient decolorization of dye water. J. Mater. Chem. A. 3 (2015) 14438-14444.
[26] H. Yang, K. Liao, H. Huang, Q. Wu, L. Wan, Z. Xu. Mussel-inspired modification of a polymer membrane for ultra-high water permeability and oil-in-water emulsion separation. J. Mater. Chem. A. 2 (2014) 10225-10230.
[27] B. D. McCloskey, H. B. Park, H. Ju, B. W. Rowe, D. J. Miller, B. J. Chun, K. Kin, B. D. Freeman. Influence of polydopamine deposition conditions on pure water flux and foulant adhesion resistance of reverse osmosis, ultrafiltration, and microfiltration membranes. Polymer. 51 (2010) 3472-3485.
[28] S. N. Ramanan, N. Shahkaramipour, T. Tran, L. Zhu, S. R. Venna, C.-K. Lim, A. Singh, P. N. Prasad, H. Lin. Self-cleaning membranes for water purification by co-deposition of photo-mobile 4, 4′-azodianiline and bio-adhesive polydopamine. J. Membr. Sci. 554 (2018) 164-174.
[29] Y. Du, W. Z. Qiu, Y. Lv, J. Wu, Z. K. Xu. Nanofiltration membranes with narrow pore size distribution via contra-diffusion-induced mussel-inspired chemistry. ACS Appl. Mater. Interf. 8 (2016) 29696-29704.
[30] J. H. Ryu, P. B. Messersmith, H. Lee. Polydopamine surface chemistry: a decade of discovery. ACS Appl. Mater. Interf. 10 (2018) 7523-7540.
[31] J. r. Liebscher, R. Mrówczyński, H. A. Scheidt, C. Filip, N. D. Hădade, R. Turcu, A. Bende, S. Beck. Structure of polydopamine: a never-ending story? Langmuir. 29 (2013) 10539-10548.
[32] Equipment and instruments or materials are identified herein to adequately specify the experimental details. Such identification does not imply recommendation by the National Institute of Standards and Technology, nor does it imply the materials are necessarily the best available for the purpose.
[33] R. Yang, K. K. Gleason. Ultrathin antifouling coatings with stable surface zwitterionic functionality by initiated chemical vapor deposition (iCVD). Langmuir. 28 (2012) 12266-12274.
[34] S. T. Weinman, M. Bass, S. Pandit, M. Herzberg, V. Freger, S. M. Husson. A switchable zwitterionic membrane surface chemistry for biofouling control. J. Membr. Sci. 548 (2018) 490-501.
[35] J. Imbrogno, M. D. Williams, G. Belfort. A new combinatorial method for synthesizing, screening, and discovering antifouling surface chemistries. ACS Appl. Mater. Interf. 7 (2015) 2385-2392.
[36] W. Yuan, A. L. Zydney. Humic acid fouling during ultrafiltration. Environ. Sci. Techn. 34 (2000) 5043-5050.
[37] W. Yang, S. Chen, G. Cheng, H. Vaisocherová, H. Xue, W. Li, J. Zhang, S. Jiang. Film thickness dependence of protein adsorption from blood serum and plasma onto poly(sulfobetaine)-grafted surfaces. Langmuir. 24 (2008) 9211-9214.

[38] The appropriate SI unit is molecular mass cutoff. However, the conventional notation, molecular weight cutoff or MWCO, has been employed for this publication as it is the accepted terminology in the field.
[39] S. Kasemset, L. Wang, Z. He, D. J. Miller, A. Kirschner, B. D. Freeman, M. M. Sharma. Influence of polydopamine deposition conditions on hydraulic permeability, sieving coefficients, pore size and pore size distribution for a polysulfone ultrafiltration membrane. J. Membr. Sci. 522 (2017) 100-115.
[40] T. Tran, Y. Tu, S. Hall-Laureano, C. Lin, M. Kawy, H. Lin. "Non-stick" membranes prepared by facile surface fluorination for water purification. Ind. Eng. Chem. Res. In press (2020).
[41] D. J. Miller, D. R. Paul, B. D. Freeman. A crossflow filtration system for constant permeate flux membrane fouling characterization. Rev. Sci. Instrum. 84 (2013) 035003.
[42] D. J. Miller, S. Kasemset, L. Wang, D. R. Paul, B. D. Freeman. Constant flux crossflow filtration evaluation of surface-modified fouling-resistant membranes. J. Membr. Sci. 452 (2014) 171-183.
[43] P. R. Bevington, D. K. Robinson. Data reduction and error analysis for the physical sciences. second ed. New York: McGraw-Hill, Inc.; 1992.
[44] P. Bengani-Lutz, R. D. Zaf, P. Z. Culfaz-Emecen, A. Asatekin. Extremely fouling resistant zwitterionic copolymer membranes with~ 1 nm pore size for treating municipal, oily and textile wastewater streams. J. Membr. Sci. 543 (2017) 184-194.
[45] S. T. Weinman, S. M. Husson. Influence of chemical coating combined with nanopatterning on alginate fouling during nanofiltration. J. Membr. Sci. 513 (2016) 146-154.
[46] Y. Baek, B. D. Freeman, A. L. Zydney, J. Yoon. A facile surface modification for antifouling reverse osmosis membranes using polydopamine under UV irradiation. Ind. Eng. Chem. Res. 56 (2017) 5756-5760.
[47] K. J. Varin, N. H. Lin, Y. Cohen. Biofouling and cleaning effectiveness of surface nanostructured reverse osmosis membranes. J. Membr. Sci. 446 (2013) 472-481.
[48] L. Zhao, W. S. W. Ho. Novel reverse osmosis membranes incorporated with a hydrophilic additive for seawater desalination. J. Membr. Sci. 455 (2014) 44-54.
[49] Y. Ye, P. Le Clech, V. Chen, A. G. Fane, B. Jefferson. Fouling mechanisms of alginate solutions as model extracellular polymeric substances. Desalination. 175 (2005) 7-20.
[50] K. Katsoufidou, S. G. Yiantsios, A. J. Karabelas. Experimental study of ultrafiltration membrane fouling by sodium alginate and flux recovery by backwashing. J. Membr. Sci. 300 (2007) 137-146.
[51] H. Chang, H. Liang, F. S. Qu, S. L. Shao, H. R. Yu, B. Liu, W. Gao, G. B. Li. Role of backwash water composition in alleviating ultrafiltration membrane fouling by sodium alginate and the effectiveness of salt backwashing. J. Membr. Sci. 499 (2016) 429-441.
[52] A. Y. Kirschner, Y.-H. Cheng, D. R. Paul, R. W. Field, B. D. Freeman. Fouling mechanisms in constant flux crossflow ultrafiltration. J. Membr. Sci. 574 (2019) 65-75.
[53] D. J. Miller, X. Huang, H. Li, S. Kasemset, A. Lee, D. Agnihotri, T. Hayes, D. R. Paul, B. D. Freeman. Fouling-resistant membranes for the treatment of flowback water from hydraulic shale fracturing: a pilot study. J. Membr. Sci. 437 (2013) 265-275.